

Improved complete ensemble EMD: A suitable tool for biomedical signal processing

Marcelo A. Colominas^{a,b}, Gastón Schlotthauer^{a,b,*}, María E. Torres^{a,b}

^a Laboratorio de Señales y Dinámicas no Lineales, Universidad Nacional de Entre Ríos, Ruta Prov. 11 Km 10.5, Oro Verde, Entre Ríos, Argentina

^b Consejo Nacional de Investigaciones Científicas y Técnicas (CONICET), Argentina



ARTICLE INFO

Article history:

Received 16 December 2013

Received in revised form 20 May 2014

Accepted 26 June 2014

Keywords:

Empirical mode decomposition (EMD)

Noise-assisted data analysis

Electroglography

Ventricular fibrillation

Epileptic seizure

ABSTRACT

The empirical mode decomposition (EMD) decomposes non-stationary signals that may stem from nonlinear systems, in a local and fully data-driven manner. Noise-assisted versions have been proposed to alleviate the so-called “mode mixing” phenomenon, which may appear when real signals are analyzed. Among them, the complete ensemble EMD with adaptive noise (CEEMDAN) recovered the completeness property of EMD. In this work we present improvements on this last technique, obtaining components with less noise and more physical meaning. Artificial signals are analyzed to illustrate the capabilities of the new method. Finally, several real biomedical signals are decomposed, obtaining components that represent physiological phenomena.

© 2014 Elsevier Ltd. All rights reserved.

1. Introduction

Empirical mode decomposition (EMD) [1] is an adaptive (data-driven) method to analyze non-stationary signals stemming from nonlinear systems. It produces a local and fully data-driven separation of a signal in fast and slow oscillations. At the end, the original signal can be expressed as a sum of amplitude and frequency modulated (AM-FM) functions called “intrinsic mode functions” (IMFs), or simply modes, plus a final monotonic trend. In this way, EMD is complete.

The local nature of the EMD may produce oscillations with very disparate scales in one mode, or oscillations with similar scales in different modes. When this phenomenon is undesirable, and similar scales for each mode are preferred, this consequence of the method becomes a problem, named as “mode mixing”. To alleviate it, a new method was proposed: the ensemble empirical mode decomposition (EEMD) [2], which performs the decomposition over an ensemble of noisy copies of the original signal, obtaining the final results by averaging. The addition of white Gaussian noise reduces the mode mixing by populating the whole time-frequency

space, taking advantage of the dyadic filter bank behavior of the EMD [3]. Thus, more regular modes are obtained, with similar scales for the whole time span. Even if EEMD has shown to be useful in a wide range of applications [4,5,16], it also created new difficulties. Indeed, as a consequence of the algorithm, the reconstructed signal, the sum of the modes and the final trend, contains residual noise. Also, different realizations of signal plus noise may produce a different number of modes, making difficult the final averaging. The Complementary EEMD [7] significantly alleviated the reconstruction problem by using complementary (i.e., adding and subtracting) pairs of noise. However, the completeness property cannot be proven, and the final averaging problem remains unsolved since different noisy copies of the signal can produce a different number of modes.

The complete ensemble empirical mode decomposition with adaptive noise (CEEMDAN) [8] proved to be an important improvement on EEMD, achieving a negligible reconstruction error and solving the problem of different number of modes for different realizations of signal plus noise. Applications of this technique can be found in areas such as biomedical engineering [9], seismology [10,11] and building energy consumption [12].

In spite of that, CEEMDAN still has some aspects in which it deserves to be improved: (i) its modes contain some residual noise; and (ii) the signal information appears “later” than in EEMD with some “spurious” modes in the early stages of the decomposition. The first two or three modes contain an important amount of noise and similar scales of the signal, as it can be seen in the signals analyzed in [8,13]. We address this two issues in the present paper.

* Corresponding author at: Laboratorio de Señales y Dinámicas no Lineales, Universidad Nacional de Entre Ríos, Ruta Prov. 11 Km 10.5, Oro Verde, Entre Ríos, Argentina. Tel.: +54 343 4975100.

E-mail addresses: macolominas@bioingenieria.edu.ar (M.A. Colominas), gschlotthauer@conicet.gov.ar (G. Schlotthauer), metorres@santafe-conicet.gov.ar (M.E. Torres).

The paper is organized as follows. In Section 2 a brief explanation about EMD, EEMD and original CEEMDAN is given. In Section 3 we introduce the improvements on CEEMDAN. Section 4 is devoted to the experiments and results discussion. Section 5 concludes the paper.

2. EMD, EEMD, complementary EEMD and CEEMDAN

The EMD technique [1] decomposes a signal into a usually small number of IMFs. To be considered as an IMF, a signal must fulfill two conditions: (i) the number of extrema (maxima and minima) and the number of zero-crossings must be equal or differ at most by one; and (ii) the local mean, defined as the mean of the upper and lower envelopes, must be zero. The algorithm can be described as follows [1]:

- Step 1. Set $k=0$ and find all extrema of $r_0=x$.
- Step 2. Interpolate between minima (maxima) of r_k to obtain the lower (upper) envelope e_{min} (e_{max}).
- Step 3. Compute the mean envelope $m=(e_{min}+e_{max})/2$.
- Step 4. Compute the IMF candidate $d_{k+1}=r_k-m$.
- Step 5. Is d_{k+1} an IMF?
 - Yes. Save d_{k+1} , compute the residue $r_{k+1}=x-\sum_{i=1}^kd_i$, do $k=k+1$, and treat r_k as input data in step 2.
 - No. Treat d_{k+1} as input data in step 2.
- Step 6. Continue until the final residue r_K satisfies some predefined stopping criterion.

The refinement process (steps 2 to 5) needed to extract every mode, requires a certain number of iterations and is named as *sifting* process.

The ensemble version, EEMD [2], defines the “true” modes as the average of the corresponding IMFs obtained from an ensemble of the original signal plus different realizations of finite variance white noise. Let x be the signal of interest. The EEMD algorithm can be described as follows:

- Step 1. Generate $x^{(i)}=x+\beta w^{(i)}$, where $w^{(i)}$ ($i=1, \dots, I$) is a zero mean unit variance white noise realization, and $\beta>0$.
- Step 2. Decompose completely each $x^{(i)}$ ($i=1, \dots, I$) by EMD, obtaining the modes $d_k^{(i)}$, where $k=1, \dots, K$ indicates the mode.
- Step 3. Assign \bar{d}_k as the k th mode of x , obtained by averaging the corresponding modes: $\bar{d}_k=\frac{1}{I}\sum_{i=1}^Id_k^{(i)}$.

The extraction of every $d_k^{(i)}$ requires a different number of *sifting* iterations.

It can be noticed that in EEMD, every $x^{(i)}$ is decomposed independently from the other realizations and for every one of them a residue $r_k^{(i)}=r_{k-1}^{(i)}-d_k^{(i)}$ is obtained at each stage, with no connection between the different realizations. This situation is the cause of some EEMD disadvantages: (i) the decomposition is not complete and (ii) different realizations of signal plus noise might produce different number of modes.

In order to deal with the reconstruction error, the complementary EEMD [7] was proposed. Noise is added in pairs to the original data (one positive and one negative) to generate two ensembles

$$\begin{bmatrix} y_1^{(i)} \\ y_2^{(i)} \end{bmatrix} = \begin{bmatrix} 1 & 1 \\ 1 & -1 \end{bmatrix} \begin{bmatrix} x \\ w^{(i)} \end{bmatrix}. \quad (1)$$

Although this proposals significantly alleviates the residual noise in the reconstructed signal, there is no guarantee that $y_1^{(i)}$ and $y_2^{(i)}$ will produce the same number of modes, making difficult the final averaging. Also, residual noise is present in the modes, as we will see in what follows.

Taking into account these drawbacks, in [8,14] the authors proposed a new ensemble method called CEEMDAN. The general idea is the following: $x^{(i)}$ are generated from x and the first mode $\tilde{d}_1=\bar{d}_1$ is computed exactly as in EEMD. Then, a unique first residue is obtained, independently from the noise realization:

$$r_1 = x - \tilde{d}_1. \quad (2)$$

After that, the first EMD mode is computed from an ensemble of r_1 plus different realizations of a particular noise. The second mode \tilde{d}_2 is defined as the average of these modes. The next residue is: $r_2=r_1-\tilde{d}_2$. This procedure continues until a stopping criterion is reached.

The next algorithm details the CEEMDAN method. Let $E_k(\cdot)$ be the operator which produces the k th mode obtained by EMD and let $w^{(i)}$ be a realization of zero mean unit variance white noise. Then:

- Step 1. For every $i=1, \dots, I$ decompose each $x^{(i)}=x+\beta_0 w^{(i)}$ by EMD, until its first mode and compute

$$\tilde{d}_1 = \frac{1}{I} \sum_{i=1}^I d_1^{(i)} = \bar{d}_1.$$

- Step 2. At the first stage ($k=1$) calculate the first residue as in Eq. (2): $r_1 = x - \tilde{d}_1$.

- Step 3. Obtain the first mode of $r_1 + \beta_1 E_1(w^{(i)})$, $i=1, \dots, I$, by EMD and define the second CEEMDAN mode as:

$$\tilde{d}_2 = \frac{1}{I} \sum_{i=1}^I E_1(r_1 + \beta_1 E_1(w^{(i)})).$$

- Step 4. For $k=2, \dots, K$ calculate the k th residue:

$$r_k = r_{(k-1)} - \tilde{d}_k. \quad (3)$$

- Step 5. Obtain the first mode of $r_k + \beta_k E_k(w^{(i)})$, $i=1, \dots, I$, by EMD until define the $(k+1)$ th CEEMDAN mode as:

$$\tilde{d}_{(k+1)} = \frac{1}{I} \sum_{i=1}^I E_k(r_k + \beta_k E_k(w^{(i)})). \quad (4)$$

- Step 6. Go to step 4 for the next k .

Iterate the steps 4 to 6 until the obtained residue cannot be further decomposed by EMD, either because it satisfies IMF conditions or because it has less than three local extrema.

Observe that, by construction of CEEMDAN, the final residue satisfies:

$$r_K = x - \sum_{k=1}^K \tilde{d}_k, \quad (5)$$

with K being the total number of modes. Therefore, the signal of interest x can be expressed as

$$x = \sum_{k=1}^K \tilde{d}_k + r_K, \quad (6)$$

ensuring the completeness property of the proposed decomposition and thus providing an exact reconstruction of the original data. The final number of modes is determined only by the data and the stopping criterion. The coefficients $\beta_k = \varepsilon_k \text{std}(r_k)$ allow the selection of the SNR at each stage.

3. Improvements on CEEMDAN

It was shown in [8] and [14] how CEEMDAN overcomes the main difficulties of EEMD, but it still has two problems, as it was stated in the Section 1. These issues, the presence of residual noise in the modes and the existence of spurious modes, are addressed in this Section.

3.1. Residual noise in modes

The main idea in the noise-assisted variations of EMD is to add some controlled noise to the signal in order to create new extrema. In this way, the local mean is “forced” to stick to the original signal in those portions where new extrema were created while it remains unmodified in the rest of the signal (where no creation of extrema occurred); i.e., the algorithm is forced to focus in some specific values of the scale-energy space. Averaging is meant to better estimate this local mean that is slightly different across the signal plus noise realizations.

However, EEMD does not estimate *local means* but *modes* instead. This is because it independently decomposes each realization of signal plus noise, so at the first stage of each realization decomposition there is one local mean and one mode. It is impossible to proceed in a different way in EEMD, then the *true mode* is an average of modes of noisy copies of the original signal, containing some residual noise.

On the other hand, CEEMDAN uses each final mode for the computation of the next one. Each mode is computed sequentially, in a deflationary scheme. Then, we can proceed differently from EEMD estimating the local means of each realization of signal plus noise and defining the *true mode* as the difference between the *current residue* and the *average of its local means*.

Let us recall the operator $E_k(\cdot)$, and let $M(\cdot)$ be the operator which produces the local mean of the signal that is applied to. It can be noticed that $E_1(x) = x - M(x)$. Let $w^{(i)}$ be a realization of white Gaussian noise, $x^{(i)} = x + w^{(i)}$, and $\langle \cdot \rangle$ the action of averaging throughout the realizations. For the first EEMD and original CEEMDAN modes we have:

$$\tilde{d}_1 = \langle E_1(x^{(i)}) \rangle = \langle x^{(i)} - M(x^{(i)}) \rangle = \langle x^{(i)} \rangle - \langle M(x^{(i)}) \rangle. \quad (7)$$

By estimating only the local mean and subtracting it from the original signal, we have:

$$\tilde{d}_1 = x - \langle M(x_i) \rangle. \quad (8)$$

In this way, we obtain a reduction in the amount of noise present in the modes. We are replacing the estimations of modes for the estimations local means, which better reflects what we have stated in the first paragraph.

3.2. Spurious modes

In the original formulation of CEEMDAN [8], we computed the first mode in the same way as in EEMD (i.e., averaging first modes of signal plus white noise). To extract the rest of the modes we must add a different noise to the current residue. That particular noise is an EMD mode of white noise. For example, to extract the second mode \tilde{d}_2 we must decompose different copies of $r_1 + E_1(w^{(i)})$, where r_1 is the first residue. This produces a strong overlapping in the scales we are focusing in for the first two modes (first one extracted adding white noise and the second one adding $E_1(w^{(i)})$). In order to reduce this overlapping, we propose here to make no direct use of white noise but use instead $E_k(w^{(i)})$ to extract the k th mode.

3.3. The new algorithm

Taking into account the two previous subsections, here we propose a new algorithm for CEEMDAN. We will make use of the already introduced operators $M(\cdot)$, $E_k(\cdot)$. Let $w^{(i)}$ be a realization of white Gaussian noise with zero mean and unit variance. With this in mind, we propose the improved CEEMDAN’s algorithm as follows:

Step 1. Calculate by EMD the local means of I realizations $x^{(i)} = x + \beta_0 E_1(w^{(i)})$ to obtain the first residue

$$r_1 = \langle M(x^{(i)}) \rangle.$$

Step 2. At the first stage ($k=1$) calculate the first mode: $\tilde{d}_1 = x - r_1$.

Step 3. Estimate the second residue as the average of local means of the realizations $r_1 + \beta_1 E_2(w^{(i)})$ and define the second mode:

$$\tilde{d}_2 = r_1 - r_2 = r_1 - \langle M(r_1 + \beta_1 E_2(w^{(i)})) \rangle.$$

Step 4. For $k=3, \dots, K$ calculate the k th residue

$$r_k = \langle M(r_{k-1} + \beta_{k-1} E_k(w^{(i)})) \rangle.$$

Step 5. Compute the k th mode

$$\tilde{d}_k = r_{k-1} - r_k,$$

Step 6. Go to step 4 for next k .

Constants $\beta_k = \varepsilon_k \text{std}(r_k)$ are chosen to obtain a desired SNR between the added noise and the residue to which the noise is added. Notice that in EEMD, the SNR between the added noise and the residue increases with the order k . This is because the energy of the noise in the k th residue, $k > 1$, is only a fraction of the energy of the noise added at the beginning of the algorithm. To emulate this behavior, in the present work we will set β_0 in a way that ε_0 is exactly the reciprocal of the desired SNR between the first added noise and the analyzed signal: if we express the SNR as a quotient of standard deviations, we have $\beta_0 = \varepsilon_0 \text{std}(x)/\text{std}(E_1(w^{(i)}))$. In order to obtain noise realizations with smaller amplitudes for the late stages of the decomposition, in the rest of the modes we will use the noise as resulting from its pre-processing by EMD, i.e., without normalizing them by its standard deviation ($\beta_k = \varepsilon_0 \text{std}(r_k)$, $k \geq 1$). Studies on the influence of this important parameter can be found in [14]. A flowchart of this new algorithm can be found in Fig. 1.

In what follows, we will refer the method introduced in [8] as original CEEMDAN and the improved version here presented as improved CEEMDAN. In all implementations we used the EMD toolbox available at: <http://perso.ens-lyon.fr/patrick.flandrin/emd.html>. An implementation of the original formulation of CEEMDAN can be found at: <http://www.bioingenieria.edu.ar/grupos/ldnlys/>.

4. Experiments and results

In this section we illustrate the abilities of the improved CEEMDAN here proposed. Analyzing the decompositions of two artificial signals, we compare the results of this method with those of EMD, EEMD, and the original CEEMDAN. Additionally, three biomedical signals are decomposed by the improved CEEMDAN (electroglottogram, electrocardiogram and electroencephalogram) in order to show some of its potential applications.

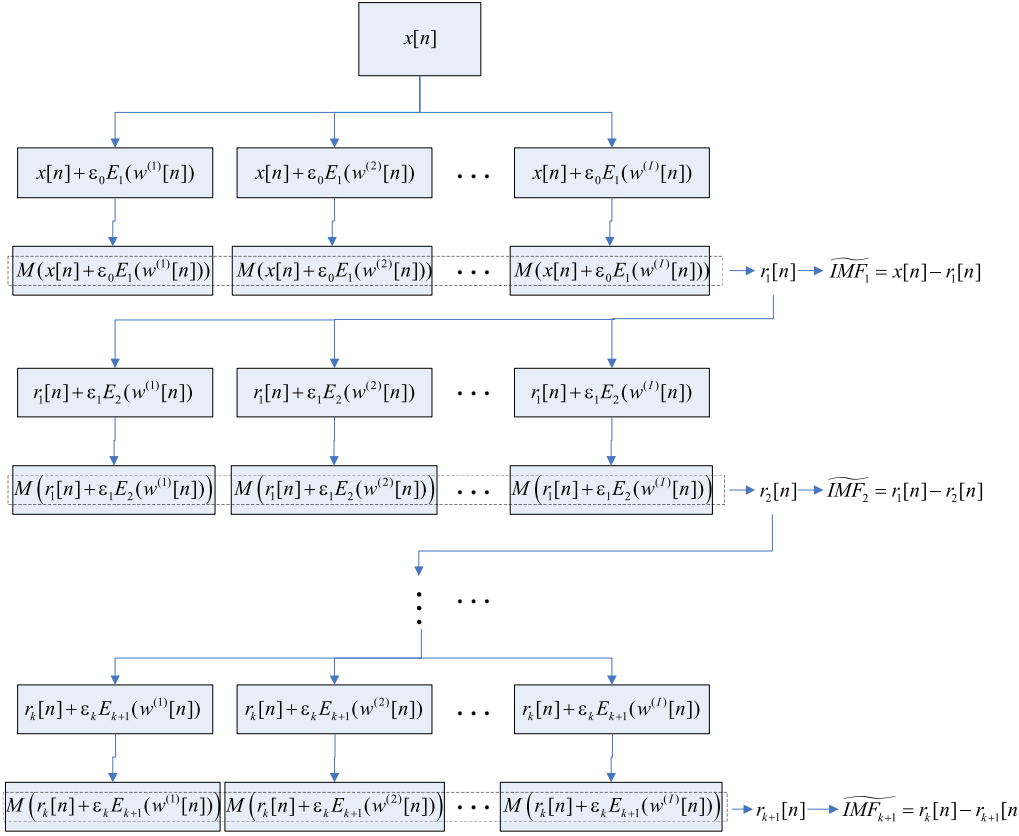


Fig. 1. Flowchart describing the improved version of CEEMDAN.

4.1. Artificial signals

As a first example, we propose here a classical mode mixing example. A sustained pure tone plus a gapped one with a higher frequency will inevitably lead us to mode mixing when analyzed via EMD, due to the local nature of the method. The analyzed signal is $s = s_1 + s_2$ with

$$s_1 = \begin{cases} 0 & \text{if } 1 \leq n \leq 500 \\ \sin(2\pi 0.255(n - 501)) & \text{if } 501 \leq n \leq 750 \\ 0 & \text{if } 751 \leq n \leq 1000. \end{cases} \quad (9)$$

$$s_2 = \sin(2\pi 0.065(n - 1)) \quad (10)$$

We present a typical decomposition for the five here analyzed methods in Fig. 2. Mode mixing is evident in EMD, with modes three onwards having very little energy and undesirable oscillations. For the three noise-assisted methods the pure tone is well recovered and also the fast component, avoiding the mode mixing. However, in EEMD every realization of signal plus noise was completely decomposed independently from each other and then a total number of nine modes was obtained, although from the third mode onwards they have very small energy, without representing information of the original signal. Exactly the same problem is experienced for Complementary EEMD. The deflationary scheme of the complete versions (original and improved CEEMDAN) allow us to evaluate an objective global stopping criterion at every stage and thus to stop sooner the decomposition, once the IMF conditions are satisfied. A “spurious” second mode appears for original CEEMDAN.

Because of the stochastic ingredient in the noise-assisted methods, different decompositions of the same signal are in fact slightly different. Also, the energy of residual noises should decrease as ensemble size I increases. In order to quantify the performances of the methods, we carried out the decompositions 100 times for the

four noise-assisted EMD variations (EEMD, Complementary EEMD, original CEEMDAN and improved CEEMDAN), and obtained statistically significant results. In each case, we used ensemble sizes of $I = 50, 100, 200, 400, 800$ ($I/2$ pairs for Complementary EEMD) and a recommended value for the noise amplitude of $\varepsilon_0 = 0.2$ [2,14].

Notice in (9) that $s_1 = 0$ for $1 \leq n \leq 500$ and $751 \leq n \leq 1000$. The fine to coarse nature of all EMD methods suggests that the fastest component (s_1 in this case) should be caught by the first mode (d_1). We measured the residual noise present in the first mode as the mean energy of the respective first modes (for all three noise-assisted methods) in those places where it is supposed to be zero. To reduce the influence of possible border effects, we considered the intervals between samples 11 and 490, and between 761 and 990. We named the mean energies of the intervals as $e_l(d_1)$ and $e_r(d_1)$ respectively.

To evaluate the capabilities of both methods to recover known components embedded in a composite signal, we use the root relative squared error of a recovered signal a with respect to a reference signal b

$$RRSE_b(a) = \frac{\|a - b\|}{\|b\|}. \quad (11)$$

The results for $e_l(d_1)$ and $e_r(d_1)$ are presented in Fig. 3. The performance of improved CEEMDAN was superimposed to those of the other three noise-assisted methods. As expected, improved CEEMDAN provides less residual noise in the first mode than EEMD and original CEEMDAN. It can be appreciated that although the noise content of Complementary EEMD first mode is lesser than that of EEMD, is still greater than the one present in improved CEEMDAN first mode. It is noteworthy that improved CEEMDAN achieves for $I=50$ a result similar to the other methods for $I=800$.

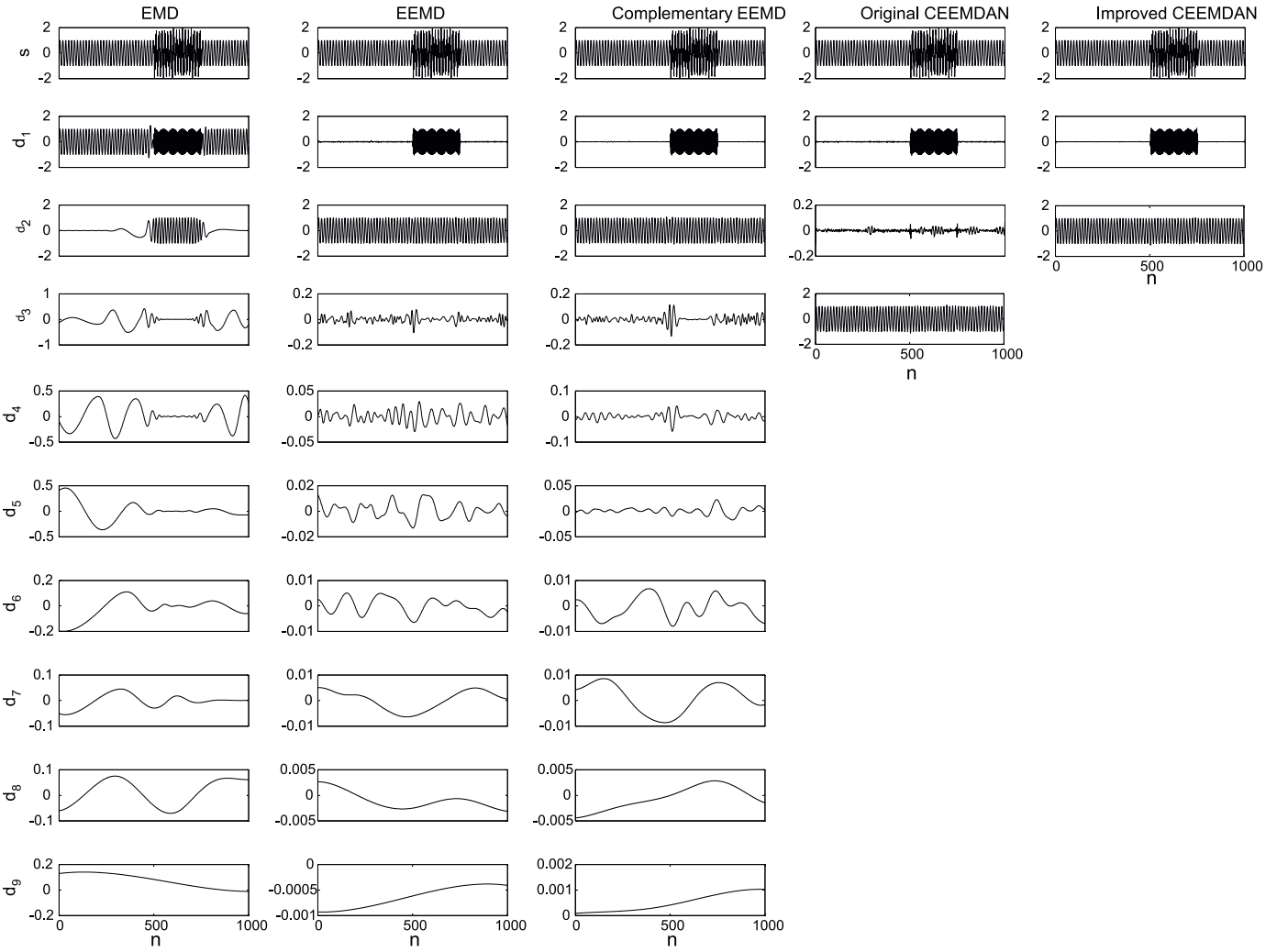


Fig. 2. Decomposition of artificial signal s by EMD, EEMD, complementary EEMD, original CEEMDAN and improved CEEMDAN.

Results of the performances when recovering known components are presented in Fig. 4. Improved CEEMDAN presents better results than the other methods. Here, the difference with Complementary EEMD is more evident, especially for the recovery of s_2 . Finally, we present the reconstruction errors in Fig. 5. As expected, the error for improved CEEMDAN is negligible when compared with that of EEMD. What is somewhat surprising is the increasing error with the ensemble size I for Complementary EEMD. These can be explained for the fact that different noisy copies of the signal produce different number of modes. Thus, as the number of realizations increases, the probability of having different number of modes increases, and so does the reconstruction error.

A more complicated artificial signal is used as a second example. It consists of two Gaussian atoms and an FM sinusoidal $x = x_1 + x_2 + x_3$, with

$$\begin{aligned} x_1 &= 3e^{-\left(\frac{n-500}{100}\right)^2} \cos\left(2\pi \frac{5}{16}(n-1000)\right), \\ x_2 &= \cos\left(2\pi \frac{f_{\max}+f_{\min}}{2}(n-1000) + \frac{f_{\max}-f_{\min}}{2} 1000 \left(\sin \frac{2\pi n}{1000} + \phi - \sin \phi\right)\right), \\ x_3 &= e^{-\left(\frac{n-1000}{200}\right)^2} \cos\left(2\pi \frac{7}{256}(n-1000)\right), \end{aligned}$$

$$\text{for } 1 \leq n \leq 1000, \quad f_{\max} = 3/32, \quad f_{\min} = 9/128 \quad \text{and} \quad \phi = -\arccos\left(\frac{3f_{\min}+f_{\max}}{f_{\max}-f_{\min}}\right)$$

The signal was decomposed via EMD, EEMD, Complementary EEMD and the original and improved versions of CEEMDAN using in all cases the recommended value for the noise amplitude of $\varepsilon_0 = 0.2$ [2,14] and an ensemble size of $I = 50$ ($I/2 = 25$ pairs for Complementary EEMD). Results for improved CEEMDAN (in black) and EEMD (in red [gray]) are presented in Fig. 6, where they were overlapped for comparison purposes, along with the frequency spectra of the improved CEEMDAN modes. It is worthy to mention the fact that the second EEMD residue was obtained by summing the modes third to last. This is because it is impossible to impose an objective global stopping criterion, since every realization of signal plus noise is decomposed independently from each other. In the case of EEMD the second residue was artificially created, summing up the modes three to last, only for comparison purposes.

It can be appreciated the data-driven filter bank behavior for EEMD and improved CEEMDAN. The signal x_1 is correctly isolated, as well as x_2 and x_3 which are very close in frequency. Although similar results can be obtained with a linear filter bank, in this case it was no necessary to specify the number of filters, nor its central frequencies, nor its bandwidths. The “spontaneously” generated filter bank separating components with different spectra with no *a priori* known distribution is a valuable property of these methods.

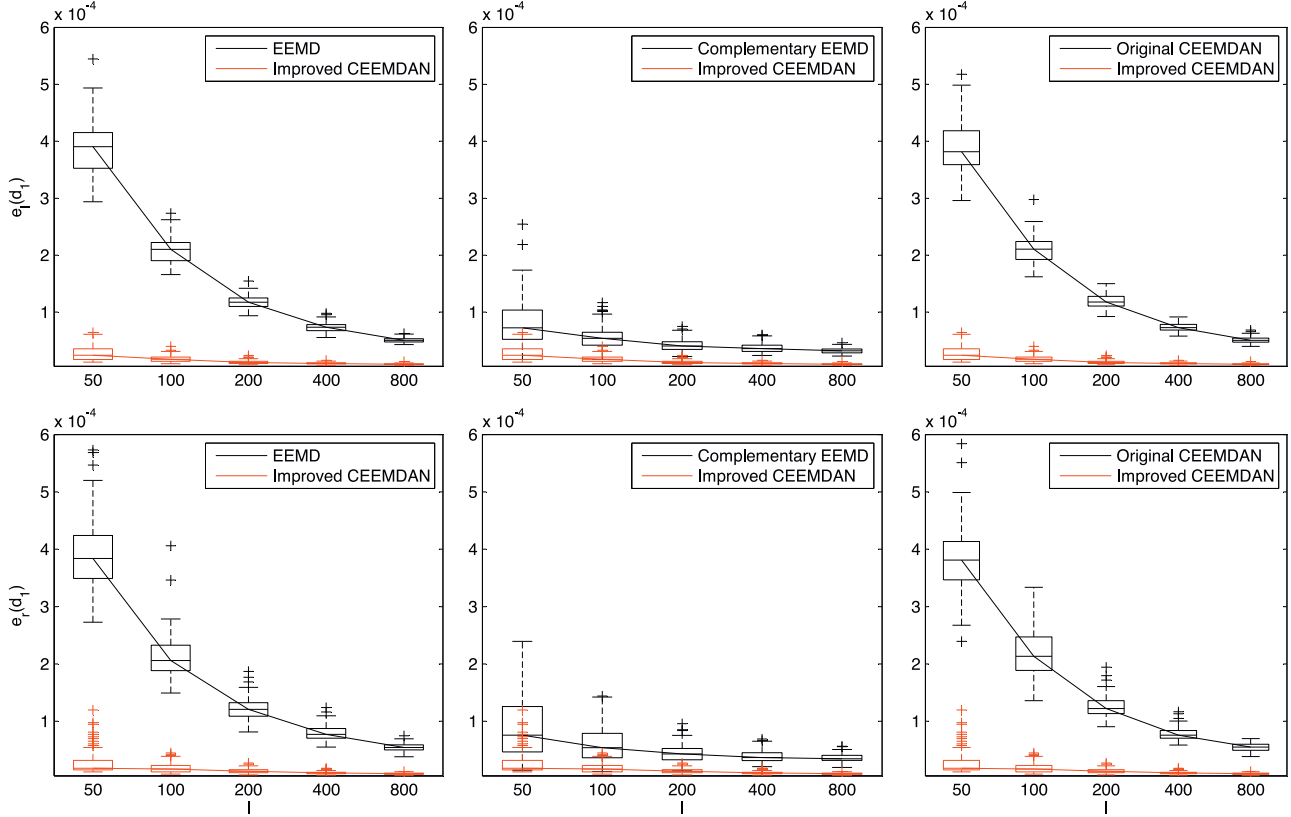


Fig. 3. Performances of the four noise-assisted methods on artificial signal s . Top row: energy of the first half of d_1 . Bottom row: energy of the last quarter of d_1 .

Full decompositions of signal x for EMD and the four noise-assisted methods are presented in Fig. 7. As before, EMD presents strong mode mixing. For EEMD and Complementary EEMD, modes four onwards have little energy and they do not represent relevant information of the signal. They appear because different realizations of signal plus noise have produced a different number of modes. The original version of CEEMDAN have produced a spurious second mode. The improved version instead, have well

recovered the three components of the original signal. As in the previous example, here it can be also appreciated that modes one and three in improved CEEMDAN contain less noise than those obtained with the other noise-assisted EMD methods. For both, original and improved CEEMDAN the decompositions were stopped once the IMF conditions were satisfied for the current residue.

We achieved a method that provides modes with less noise and avoids the spurious modes present in the original formulation of

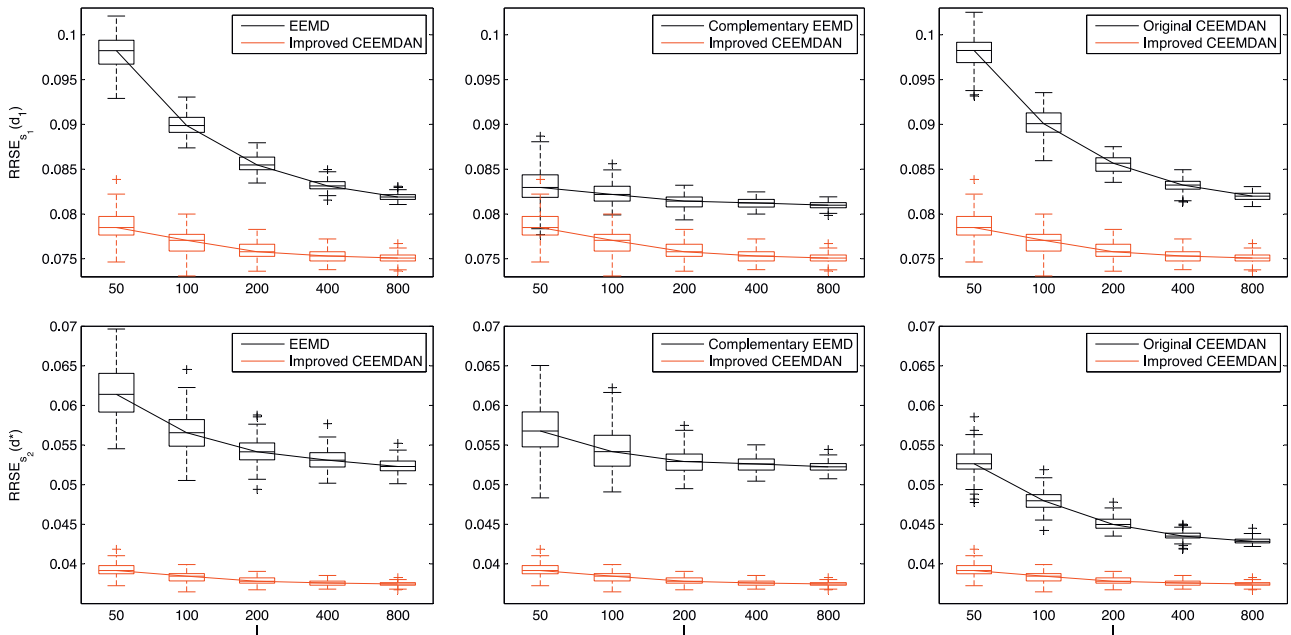


Fig. 4. Performances of the four noise-assisted methods on artificial signal s . Top row: error when recovering s_1 . Bottom row: error when recovering s_2 .

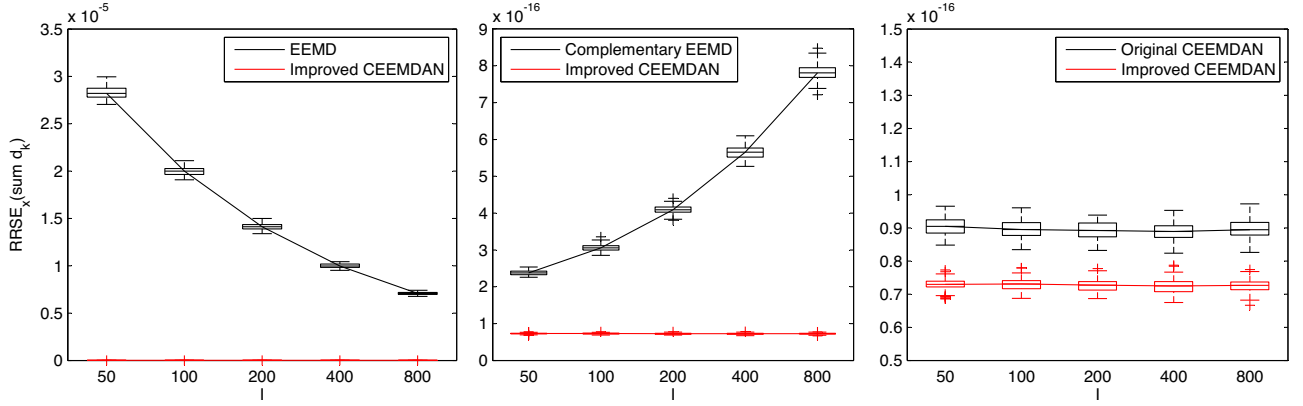


Fig. 5. Performances of the four noise-assisted methods on artificial signal *s*: reconstruction error.

CEEMDAN. We will next apply the improved version of CEEMDAN to several biomedical signals, illustrating its potential as an analysis tool for this kind of applications.

4.2. Electroglottogram

The electroglottograph (EGG) is a very widespread technique which allows the investigation of the contact area of the phonating vocal folds, in a simple and non-invasive way. It is characterized by an increasing in the amplitude of the signal in the glottal closing instant [15]. Its study allows a fundamental frequency tracking in voiced phonemes. Therefore, it would be desirable to have a noise and trend free signal to better estimate the glottal opening and closing instants.

A segment of an EGG signal from the Keele database [16] can be appreciated in Fig. 8. Its fifth improved CEEMDAN mode was superimposed. The parameters were $\varepsilon_0 = 0.2$ and $I = 100$. Also, the spectra from both signals are shown, and it can be noted that the energy present in the low frequency part of the signal (trend) is as high as the energy present in the fundamental frequency. The

improved CEEMDAN method captures in only one mode most part of the signal information, preserving important waveform features as a slightly asymmetry, where the increasing in the amplitude due to the glottal closure is faster than the decreasing in the amplitude due to the opening [15]. All modes of the decomposition are shown in Fig. 9. The first two modes contain mainly noise, and the sixth mode onwards capture the low frequency content present in the trend of the signal. Valuable high frequency information associated to the closing of the vocal folds appears in the third mode, and also in the fourth with less relevance.

A different EGG signal with a clear trend from the same database is shown in the top plot of Fig. 10. As before, we have superimposed its fifth improved CEEMDAN mode. Same values for the parameters were used. In this case, the energy of the fundamental frequency is much smaller than the energy of the low frequency noise, and still improved CEEMDAN captures in one mode the most important information of the signal, preserving waveform characteristics. Moreover, a decreasing in the frequency of the signal which is perfectly caught in the fifth mode, as it can be observed. All modes are shown in Fig. 11. While the first mode contains mainly noise,

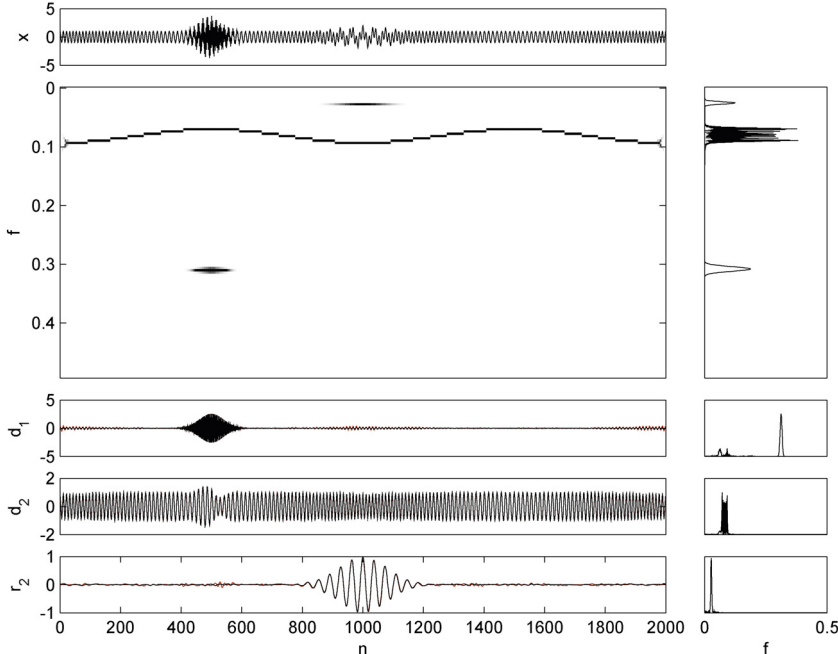


Fig. 6. Artificial signal *x*, with its reassigned spectrogram and marginal spectrum. EEMD (in red [gray]) and improved CEEMDAN (in black) results are shown along with marginal improved CEEMDAN spectra. (For interpretation of the references to color in this figure legend, the reader is referred to the web version of this article.)

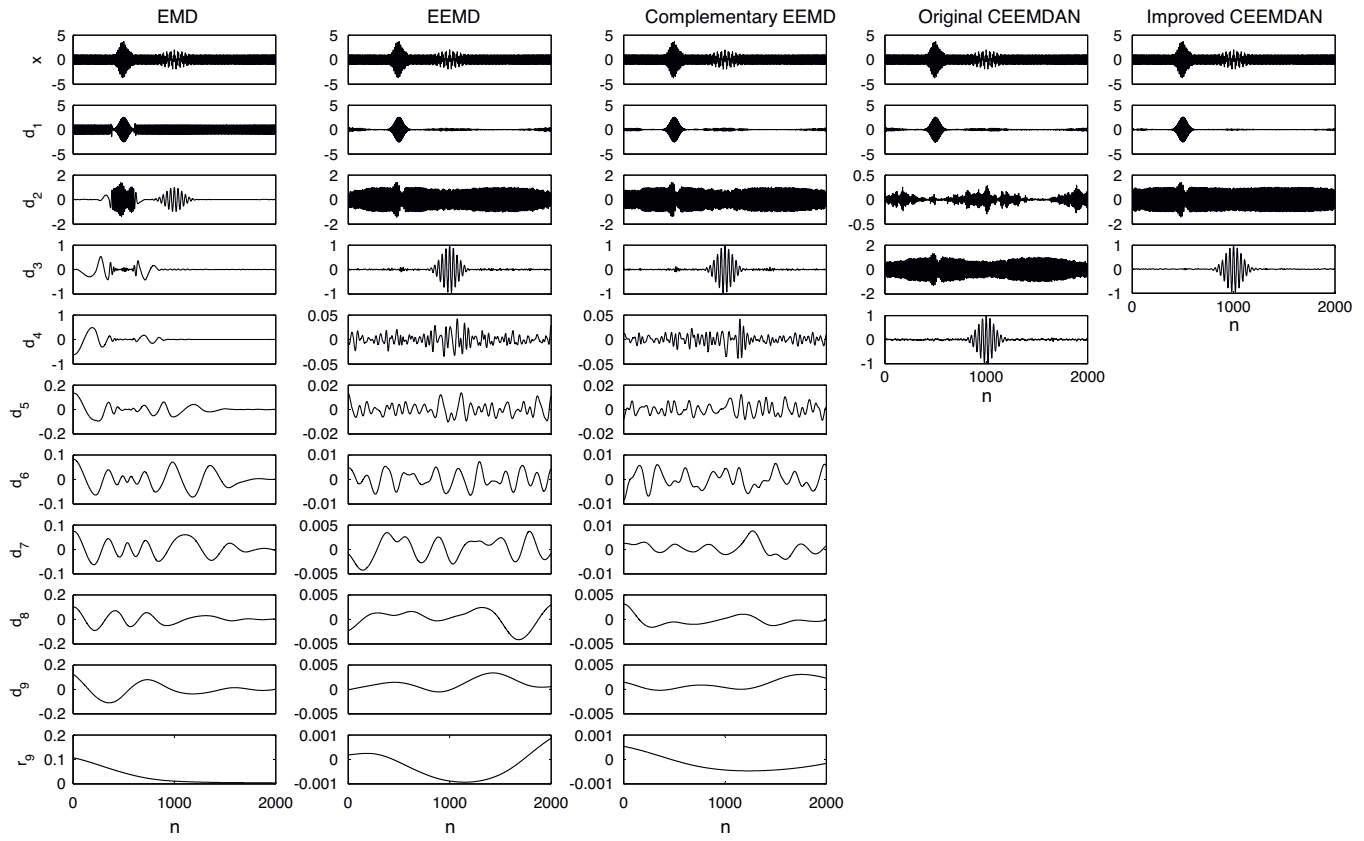


Fig. 7. Decomposition of artificial signal x by EMD, EEMD, complementary EEMD, original CEEMDAN and improved CEEMDAN.

the modes sixth onwards capture the trend of the signal. The third mode contains high frequency information associated to the closing of the vocal folds. The clear trend mentioned before is well captured by the last mode.

In these two examples we have illustrated the capabilities of improved CEEMDAN for data-driven filtering EGG signals. The information related to the fundamental frequency appears in only one mode. High frequency related to the glottal closure is revealed on the obtained modes.

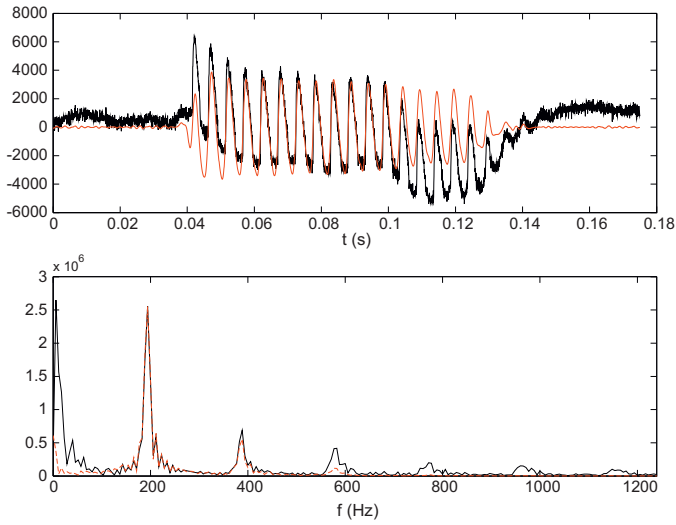


Fig. 8. Top: EGG signal (black) and fifth improved CEEMDAN mode (red [gray]). Bottom: amplitude spectra of EGG (black) and fifth improved CEEMDAN mode (red [gray]). (For interpretation of the references to color in this figure legend, the reader is referred to the web version of this article.)

4.3. Electrocardiogram with ventricular fibrillation

In most cases, the mechanism of sudden cardiac arrest onset is a ventricular tachycardia that rapidly progresses to ventricular fibrillation [17]. One third of these patients could survive with the timely employment of a defibrillator. Hence, automatic detection

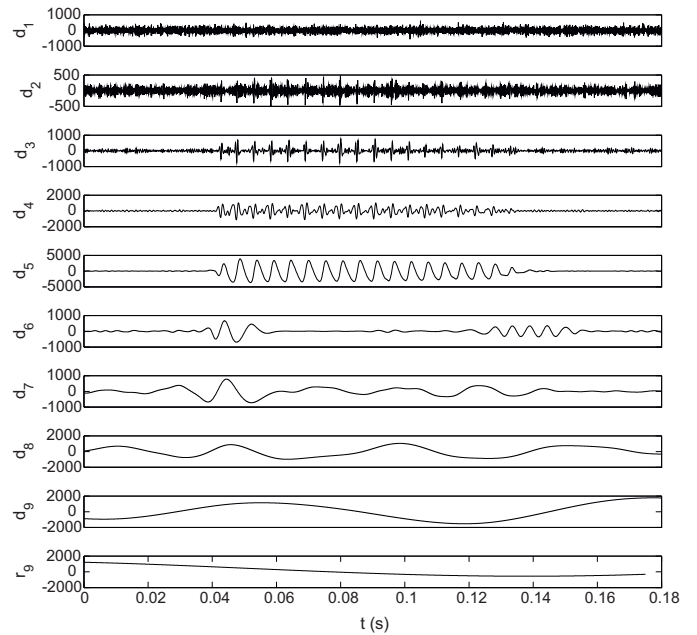


Fig. 9. Improved CEEMDAN decomposition of the EGG signal shown in Fig. 8. $\varepsilon_0 = 0.2$. $I = 100$.

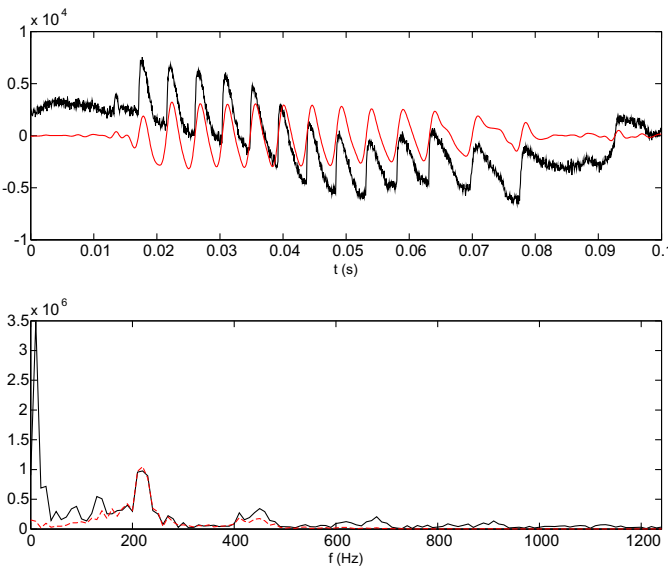


Fig. 10. Top: EGG signal (black) and fifth improved CEEMDAN mode (red [gray]). Bottom: amplitude spectra of EGG (black) and fifth improved CEEMDAN mode (red [gray]). (For interpretation of the references to color in this figure legend, the reader is referred to the web version of this article.)

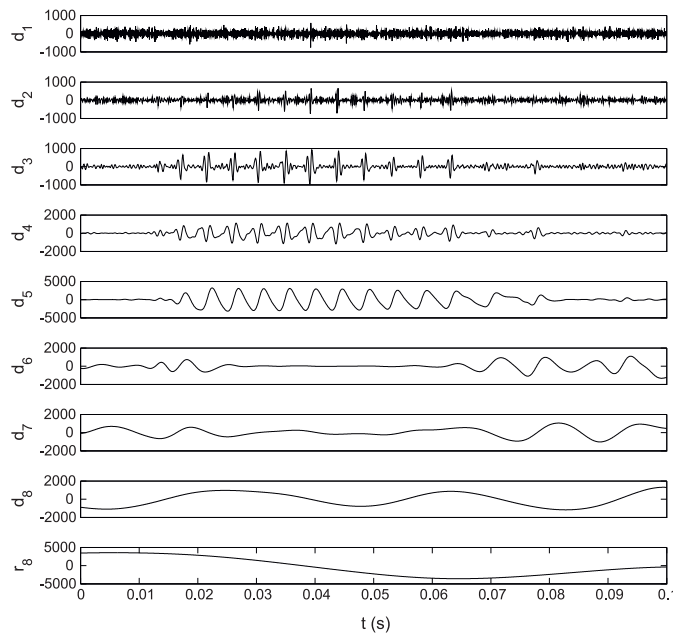


Fig. 11. Improved CEEMDAN decomposition of the EGG signal shown in Fig. 10. $\varepsilon_0 = 0.2$, $I = 100$.

of these events by analyzing electrocardiogram (ECG) signals is of vital importance [18].

A segment of an ECG record from the Creighton University (CU) ventricular tachyarrhythmia database¹ is shown in Fig. 12. The fibrillation event starting at the half of its length can be appreciated. The second improved CEEMDAN mode was superimposed. It must be noticed how this mode identifies the heart beats (QRS complexes) for the first half of the signal, while remains almost zero for the second half where no heart beat occurs. This mode is a reliable heart beat detector and could be used to identify the moments of ventricular fibrillation, characterized for the lack of beats. The

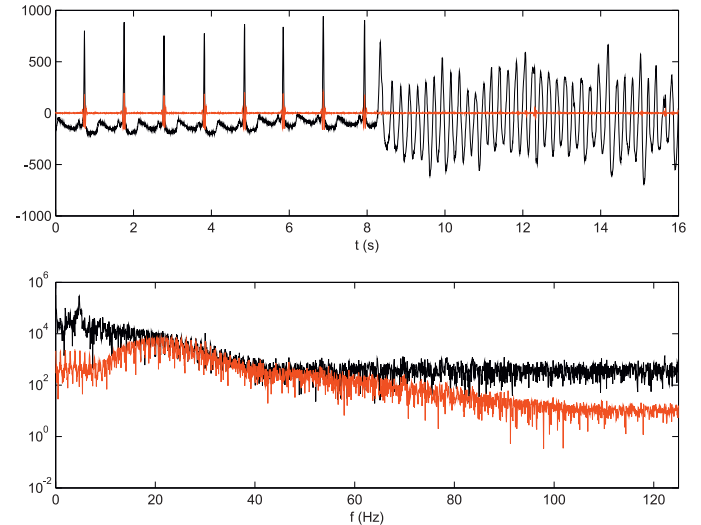


Fig. 12. Top: ECG signal (black) and second improved CEEMDAN mode (red [gray]). Bottom: amplitude spectra of EGG (black) and second improved CEEMDAN mode (red [gray]). (For interpretation of the references to color in this figure legend, the reader is referred to the web version of this article.)

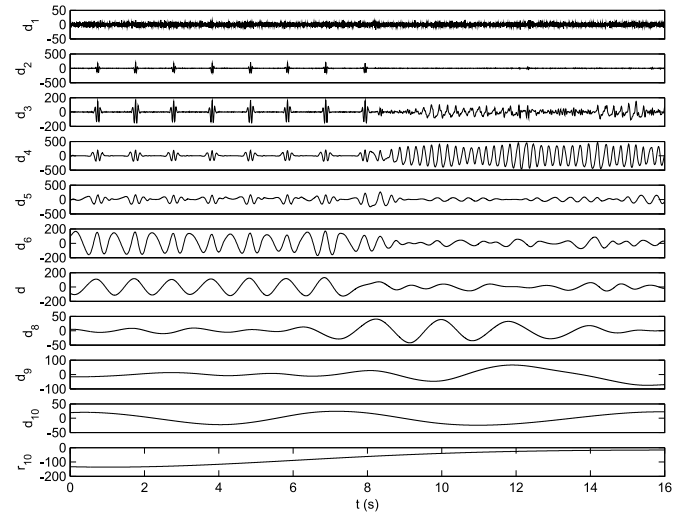


Fig. 13. Improved CEEMDAN decomposition of the ECG signal shown in Fig. 12. $\varepsilon_0 = 0.2$, $I = 100$.

spectra of both the ECG and its second improved CEEMDAN mode are also shown in Fig. 12. Although the mode contains mainly high frequencies, its energy is spread all over the spectrum, and a simple high pass or band pass filtering of the original signal cannot retrieve it.

All modes of the decomposition are presented in Fig. 13. The fourth mode contains the most part of the fibrillation event information. The first half of seventh mode captures almost perfectly the fundamental frequency of the heart, while its second half evidences the lost of sinus rhythm.

4.4. Electroencephalogram with epileptic seizure

The electroencephalograph (EEG) is a testing method that contains very useful information relating to the different physiological states of the brain [19]. Sudden crisis such as epileptic seizures are reflected on EEG recordings, and then they are suitable for automatic detection.

¹ Available at www.physionet.org

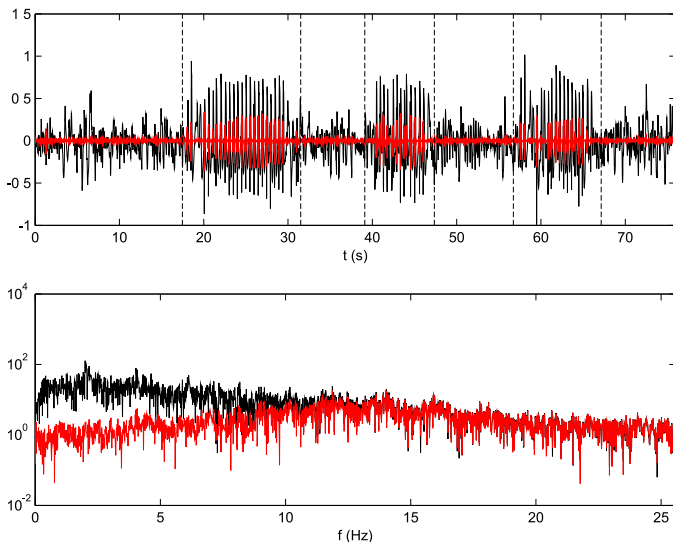


Fig. 14. Top: EEG signal (black) and first improved CEEMDAN mode (red [gray]). Bottom: amplitude spectra of EGG (black) and first improved CEEMDAN mode (red [gray]). (For interpretation of the references to color in this figure legend, the reader is referred to the web version of this article.)

A real physiological signal recorded using stereo electroencephalography (EEG) with eight multilead electrodes (2 mm long and 1.5 mm apart) was studied. It was filtered and amplified using a 1–40 Hz band pass filter. A four pole Butterworth filter was used as antialiasing low pass filter. This signal was digitized at 256 Hz through a 10 bits A/D converter. A physician accomplished the analysis of pre-ictal and ictal data by visual inspection of the EEG record. According to the visual assessment of the EEG seizure recording, the patient presented an epileptogenic area in the hippocampus with immediate propagation to the *girus cingular* and the supplementary motor area, on the left hemisphere.

The intracranial EEG recording is shown in Fig. 14, where the starting and ending moments of three epileptic seizure were marked with vertical lines. The first improved CEEMDAN mode was superimposed in red (gray). This mode seems to identify the

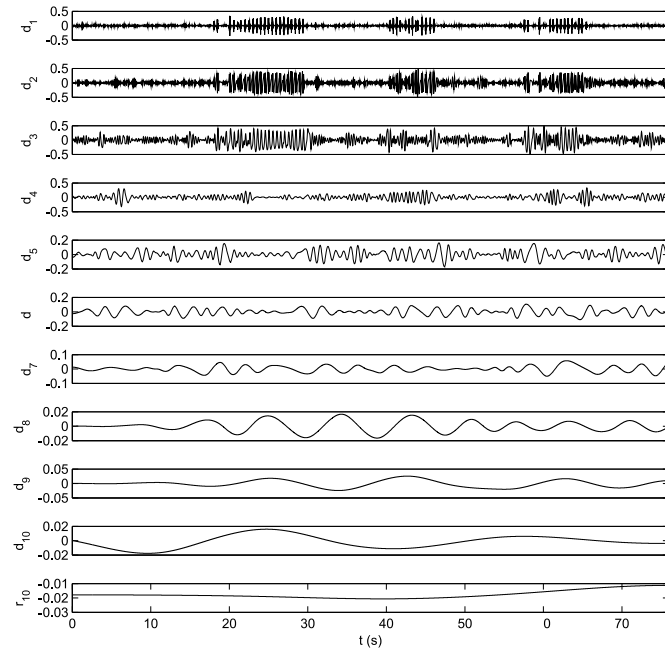


Fig. 15. Improved CEEMDAN decomposition of the EEG signal shown in Fig. 14. $\varepsilon_0 = 0.2$. $I = 100$.

seizures, and its analysis (with tools such as complexity measures [20,21]) can lead to automatic detection. From the spectra, it can be appreciated that the mode cannot be retrieved by a simple high pass filtering. All modes of the decomposition are shown in Fig. 15.

5. Conclusions

We proposed two major improvements on the CEEMDAN method. The avoidance of the spurious modes and the reduction in the amount of noise contained in the modes are important features which grant more physical meaning to the obtained results.

In general, the addition of noise sets a *global* reference for the EMD method. Then, the noise-assisted variations of EMD are less local and less data-driven (because they are also driven by the noise) than noiseless version.

We have shown the capabilities of the improved CEEMDAN method on artificial signals, confirming the theoretical improvements with respect to the original formulation. We have also illustrated the potentiality in the analysis of real biomedical signals, extracting relevant information associated with physiological processes of the systems involved in its production.

Finally, we propose this improvement to become the new standard for CEEMDAN and a reference method for the noise-assisted variation of empirical mode decomposition.

Acknowledgements

This work was supported by the Argentine National Agency for Scientific and Technological Promotion (ANPCyT-Argentina) under grant PICT-2012 2954, Universidad Nacional de Entre Ríos (Argentina) under grant PID 6136, and the Argentine National Scientific and Technical Research Council (CONICET-Argentina).

References

- [1] N.E. Huang, Z. Shen, S.R. Long, M.C. Wu, H.H. Shih, Q. Zheng, N. Yen, C.C. Tung, H.H. Liu, The empirical mode decomposition and the Hilbert spectrum for nonlinear and non-stationary time series analysis, Proc. R. Soc. Lond. A 454 (1998) 903–995.
- [2] Z. Wu, N.E. Huang, Ensemble empirical mode decomposition: a noise-assisted data analysis method, Adv. Adapt. Data Anal. 1 (1) (2009) 1–41.
- [3] P. Flandrin, G. Rilling, P. Gonçalves, Empirical mode decomposition as a filter bank, IEEE Signal Process. Lett. 11 (2) (2004) 112–114.
- [4] Y. Lei, Z. He, Y. Zi, Application of the EEMD method to rotor fault diagnosis of rotating machinery, Mech. Syst. Signal Process. 23 (4) (2009) 1327–1338.
- [5] Z. Wu, E.K. Schneider, B.P. Kirtman, E.S. Sarachik, N.E. Huang, C.J. Tucker, The modulated annual cycle: an alternative reference frame for climate anomalies, Clim. Dyn. 31 (7–8) (2008) 823–841.
- [6] G. Schlotthauer, M.E. Torres, H. Rufiner, A new algorithm for instantaneous f_0 speech extraction based on ensemble empirical mode decomposition, in: 17th Eur. Signal Process. Conf. 2009, Glasgow, Scotland, United Kingdom, 2009, pp. 2347–2351.
- [7] J.-R. Yeh, J.-S. Shieh, N.E. Huang, Complementary ensemble empirical mode decomposition: a novel noise enhanced data analysis method, Adv. Adapt. Data Anal. 2 (02) (2010) 135–156.
- [8] M.E. Torres, M.A. Colominas, G. Schlotthauer, P. Flandrin, A complete ensemble empirical mode decomposition with adaptive noise, in: Proc. 36th IEEE Int. Conf. on Acoust., Speech and Signal Process., ICASSP 2011, Prague, Czech Republic, 2011, pp. 4144–4147.
- [9] X. Navarro, F. Poree, G. Carrault, ECG removal in preterm EEG combining empirical mode decomposition and adaptive filtering, in: Proc. of the 37th IEEE Int. Conf. on Acoust., Speech and Signal Process., ICASSP 2012, IEEE, 2012, pp. 661–664.
- [10] J. Han, M. van der Baan, Empirical mode decomposition for seismic time-frequency analysis, Geophysics 78 (2) (2013) 09–019.
- [11] A. Hooshmand, J. Nasseri, H.R. Siahkoohi, Seismic data denoising based on the complete ensemble empirical mode decomposition, in: Int. Geophysical Conf. and Oil & Gas Exhibition, Istanbul, Turkey, 2012, pp. 1–4.
- [12] R. Fontugne, J. Ortiz, N. Tremblay, P. Borgnat, P. Flandrin, K. Fukuda, D. Culler, H. Esaki, Strip, bind, and search: a method for identifying abnormal energy consumption in buildings, in: Proc. of the 12th Int. Conf. on Inf. Process. in Sens. Netw., ACM, 2013, pp. 129–140.
- [13] M.A. Colominas, G. Schlotthauer, P. Flandrin, M.E. Torres, Descomposición empírica en modos por conjuntos completos con ruido adaptativo y aplicaciones

- biomédicas, in: XVIII Congreso Argentino de Bioingeniería y VII Jornadas de Ingeniería Clínica, Mar del Plata, Argentina, 2011.
- [14] M.A. Colominas, G. Schlotthauer, M.E. Torres, P. Flandrin, Noise-assisted EMD methods in action, *Adv. Adapt. Data Anal.* 04 (04) (2012) 1250025.
 - [15] N. Henrich, C. d'Alessandro, B. Doval, M. Castellengo, On the use of the derivative of electroglottographic signals for characterization of nonpathological phonation, *J. Acoust. Soc. Am.* 115 (3) (2004) 1321–1332.
 - [16] F. Plante, G.F. Meyer, W.A. Ainsworth, A pitch extraction reference database, in: 4th Eur. Conf. on Speech Commun. and Technol., Madrid, Spain, 1995, pp. 837–840.
 - [17] A. Amann, R. Tratnig, K. Unterkofler, et al., Reliability of old and new ventricular fibrillation detection algorithms for automated external defibrillators, *BioMed. Eng. Online* 4 (60) (2005).
 - [18] A. Amann, R. Tratnig, K. Unterkofler, Detecting ventricular fibrillation by time-delay methods, *IEEE Trans. Biomed. Eng.* 54 (1) (2007) 174–177.
 - [19] H. Ocak, Automatic detection of epileptic seizures in EEG using discrete wavelet transform and approximate entropy, *Expert Syst. Appl.* 36 (2) (2009) 2027–2036.
 - [20] M. Añino, M. Torres, G. Schlotthauer, Slight parameter changes detection in biological models: a multiresolution approach, *Phys. A: Stat. Mech. Appl.* 324 (3) (2003) 645–664.
 - [21] M. Torres, M. Añino, G. Schlotthauer, Automatic detection of slight parameter changes associated to complex biomedical signals using multiresolution q-entropy, *Med. Eng. Phys.* 25 (10) (2003) 859–867.